International Journal of Earth Sciences Knowledge and Applications
journal homepage: http://www.ijeska.com/index.php/ijeska
e-ISSN: 2687-5993

Research Article https://doi.org/10.5281/zenodo.19919162

An Analytical Geothermal Model and Its Implications for Geothermal Engineering Design

Erlong Yang[1], James J. Sheng[2]*

[1]Northeast Petroleum University, Daqing 163318, Heilongjiang, China
[2]Texas Tech University, Lubbock, TX 79409, USA

INFORMATION

Article history
Received 06 January 2026
Revised 22 February 2026
Published 30 April 2026

Contact
*J. J. Sheng
james.sheng@ttu.edu (JJS)

How cite
Yang E., Sheng, J.J., 2026. An Analytical Geothermal Model and its Implications for Geothermal Engineering Design. *International Journal of Earth Sciences Knowledge and Applications* 8 (1), 14-22. https://doi.org/10.5281/zenodo.19919162.

Abstract
This study presents an analytical model to predict the temperature of the produced fluid and the cumulative heat production from a geothermal reservoir by cycling cold water injection. First, the solutions of the temperature of the produced fluid, the net heat production rate and the cumulative heat production are derived. Then each parameter of the analytical model is analyzed to study the sensitivity and the implications of designing a geothermal project. The derived solutions may be further used to develop other solutions or methods for geothermal engineering. From the quantitative analysis of model results, it is found that a waiting time of year is needed to produce heat until injected water breaks through in a dry geothermal system. After the breakthrough, the temperature of produced fluid is low compared to the initial reservoir temperature. This reduces the heat output. To improve that, the production rate must be high, but the residence time must be long. From that point of view, when designing a practical project, a horizontal well is preferred because of a high rate, and a large well spacing is preferred because of longer residence time. Formation thickness or injected fluid temperature does not affect the heat production significantly, but thermal conductivity does.

Keywords
Geothermal, Heat transfer, Clean energy, Heat conduction, Sustainability

Nomenclature

b : Half of injection (water) layer thickness, m
C : Heat capacity, kJ/(kg·°C)
L : Distance from the injector to the producer, m
q_h : Heat production rate, kJ/s
Q_h : Cumulative Heat Production, kJ
q_w : Water injection rate, kg/s
t : Injection time, s
T : Temperature, °C
T_{I0} : Initial injection layer temperature, °C
T_{IL} : Injection layer temperature at the production end, °C
T_i : Injection temperature, °C
v_w : Injection velocity, m/s
w : Injection (water) layer width, m
x : Distance from the injection well, m
ϑ : $(\rho C)_1/(\rho C)_2$
λ : Thermal conductivity of oil layers, kJ/(s·m·K)
ξ : Dimensionless distance
ρ : Density, kg/m^3
(ρC) : Heat capacity, kJ/(m^3·°C)
τ : Dimensionless time

Subscripts
1 : Injection (water) layer
2 : Overburden or underburden layer
bk : Breakthrough
h : Heat
i : Injection
L : At the production end
n : Time step
w : Water

1. Introduction

Because of concerns of climate change, other geoenergies that are clean and sustainable such as hydrogen energy (Sheng, 2024) and geothermal energy attract more and more attention. Geothermal energy is considered as a sustainable clean energy that can support long-term energy needs while reducing carbon emissions (Chu and Majumdar, 2012; Anderson and Rezale, 2019). Because of the strong similarity in petroleum engineering and geothermal engineering, techniques used in petroleum engineering are used to solve geothermal problems.

Martin (1975) first introduced the principles laying the foundation for advancements such as simulation tools tailored to geothermal engineering challenges like temperatures and multiphase flow. Pritchett (1995) made contributions by using STAR software to model geothermal applications crucial for optimizing production strategies. Falcone and Teodoriu (2008) pointed out transferring petroleum technology to exploration of geothermal energy for a beneficial relationship in technological progress. In particular, many authors used simulation approach. Pritchett (1995) and O'Sullivan et al. (2001) used modeling tools to optimize heat production from geothermal reservoirs. Ganguly et al. (2015) modeled reservoir temperature decline after cold water injection. Kelkar et al. (2016) used stimulation and staged development methods to effectively generate power while keeping thermal drawdown to a minimum. Bin Sultan and Sheng (2025) compared the performance of working fluids of water and CO_2 using simulation approach. However, not many publications deal with analytical solutions in geothermal reservoirs. Birhanu et al. (2023) used analytical and numerical solutions of radially symmetric aquifer thermal energy storage problems to calculate the recovery factor of the system with a cyclic repetition of injection and pumping. Chen et al. (2024) developed an analytical solution-based model using machine-learning-assisted long-term G functions for bidirectional aquifer thermal energy storage system operation. Zhang et al. (2025) studied temperature variation with depth analytically.

This study presents an analytical model to predict the temperature variation from the injection side to the production side, the temperature of the produced fluid and the cumulative heat production from a geothermal reservoir by cycling cold water injection, based on a hot water injection model. First, the analytical model and the solutions of the temperature of the produced fluid, the net heat production rate and the cumulative heat production are derived, followed by the study the effect of each parameter of the analytical model on heat production and the implications regarding how to design a geothermal project from these effects.

2. An Analytical Model and Solutions

In thermal recovery of viscous oil, hot steam or water is injected into heat oil and oil viscosity is reduced. In a geothermal process, cold water or fluid is injected into the hot geothermal reservoir to produce heat. The two processes are analogous but opposite. Lauwerier (1955) worked out the temperature distribution of the former process. This paper is to develop an analytical model from the Lauwerier (1955) solution to study geothermal processes. First, the Lauwerier model and the solution are briefly presented.

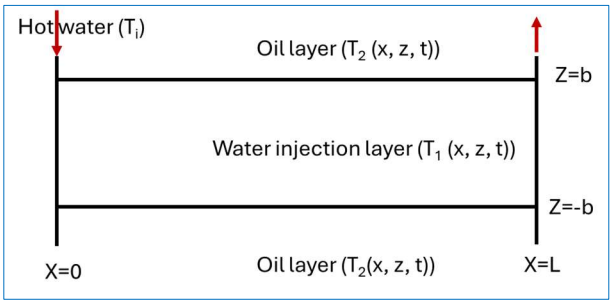

Fig. 1. Schematic of the reservoir model

Table 1. Rock and fluid properties of the base model

Parameter	Value	References
Injection temperature, T_i, °C	250	
Thermal conductivity of oil layers, λ_2, kJ/(s·m·K)	0.003	Pruess and Narasimhan, 1985
Water layer heat capacity, $(\rho C)_1$, kJ/(m^3·°C)	2600	Tadema and Weijdema, 1970
Oil layer heat capacity, $(\rho C)_2$, kJ/(m^3·°C)	2600	Tadema and Weijdema, 1970
Water heat capacity, C_w, kJ/(kg·°C)	4.1	www.engineeringtoolbox.com
half of water layer thickness, b, m	125	
Water layer width, w, m	500	
Distance from injectors to producers, L, m	500	June, 2013
Injection rate, kg/s	100	Jung, 2013
Reservoir water density, kg/m^3	800	www.engineeringtoolbox.com
The following items are calculated from the above input data:		
Water heat capacity, $(\rho C)_w$, kJ/(m^3·°C)	3280	
$\theta = (\rho C)_1/(\rho C)_2$	1	
Injection velocity, v_w, m/s	4.00E-06	
τ/t, 1/s	7.384E-11	
Breakthrough time t_{bt}, s	1.25E+08	
Breakthrough time t_{bt}, years	3.96	
τ at breakthrough, τ_{bt}, dimensionless	0.0092308	
ξ/x, 1/m	1.463E-05	
ξ_L (ξ at L), dimensionless	0.0073171	
T_{1L}, temperature at L, °C	226.5	

The reservoir model is schematically shown in Fig. 1. It is a linear model where a line of injection wells aligns in the left at x = 0, and a line of production wells aligns in the right at x = L. Hot water is injected in the middle layer with the thickness 2b, and oil layers overlies and underlies the water injection layer. Note the water layer becomes the geothermal reservoir layer, and the oil layers become the overburden and underburden layers in a geothermal system. The initial temperature of the layers (water layer and oil layers) is 0 (T_1 (x, z, t=0) = T_2 (x, z, t=0) = 0). It is assumed that heat conduction does not occur in the horizontal (X) direction, and T_1 and T_2 are functions of x, z, and t. The temperature of injected water is T_i.

$$(\rho C)_1 \frac{\partial T_1}{\partial t} + b(\rho C)_w v_w \frac{\partial T_1}{\partial x} - \lambda_2 \left(\frac{\partial T_1}{\partial t}\right)_{z=b} = 0 \quad (1)$$

$$(\rho C)_1 = (1-\phi)(\rho C)_s + \phi(1-S_{or})(\rho C)_w + \phi S_{or}(\rho C)_o \quad (2)$$

The heat balance in either of the oil layers is

$$\lambda_2 \left(\frac{\partial^2 T_2}{\partial z^2}\right) = (\rho C)_2 \frac{\partial T_2}{\partial t} \quad (3)$$

$$(\rho C)_2 = (1-\phi)(\rho C)_s + \phi(1-S_{wc})(\rho C)_o + \phi S_{wc}(\rho C)_w \quad (4)$$

Lauwerier (1955) provided the solution for the temperature distribution in the water layer:

$$T_1 = T_0 erfc\left(\frac{\xi}{2\sqrt{\theta(\tau-\xi)}}\right), when\ \tau > \xi \quad (5)$$

where $\theta = (\rho C)_1/(\rho C)_2$,

$$\tau = \frac{\lambda_2 t}{b^2(\rho C)_1} \quad (6)$$

$$\xi = \frac{\lambda_2 x}{b^2(\rho C)_w v_w} \quad (7)$$

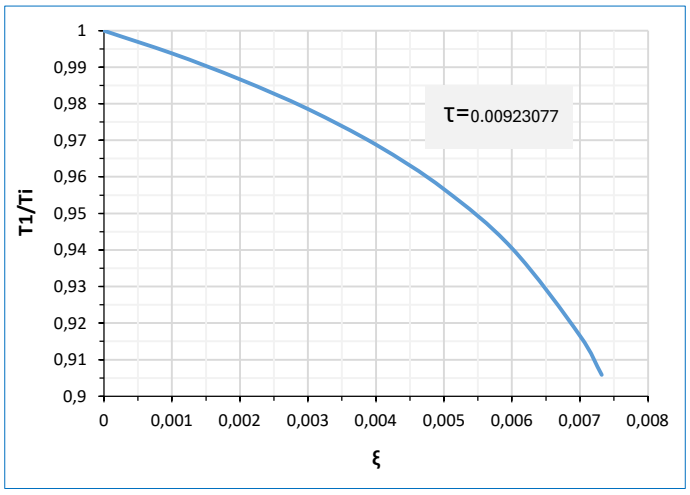

Fig. 2 Dimensionless temperature at the producer end T_1/T_i versus dimensionless distance ξ at the dimensionless breakthrough time τ = 0.0092308

Using the parameters of a base model in Table 1, for an injection rate of 100 kg/s, the hot water breakthrough time is 3.96 years, and the breakthrough temperature is 226.5 °C.

The dimensionless temperature T_1/T_i versus the dimensionless distance ξ at the dimensionless breakthrough time τ = 0.0092308 is presented in Fig. 2, and the corresponding temperature T_1 versus the distance x at the breakthrough time of 3.96 years is presented in Fig. 3.

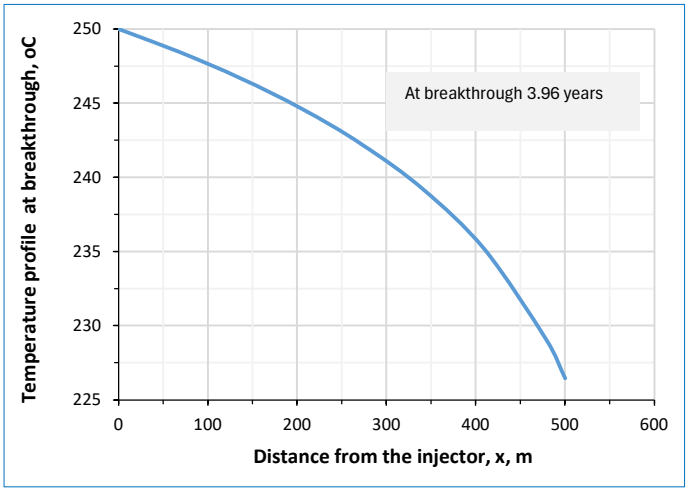

Fig. 3 Temperature at the producer end T_1 versus distance x at the breakthrough time 3.96 years

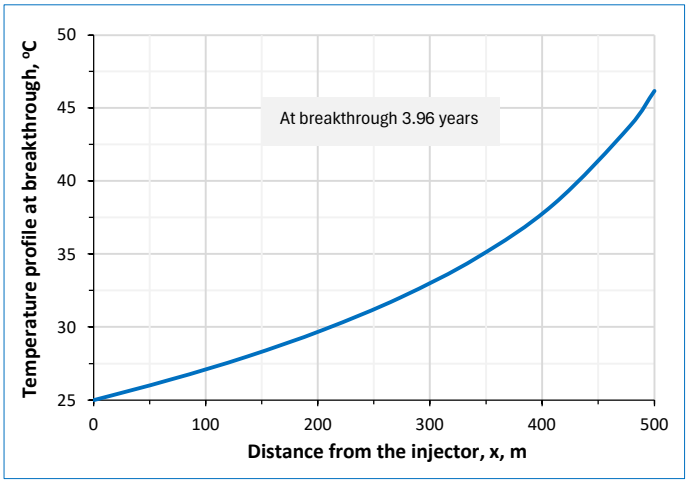

Fig. 4 Temperature T_1 versus distance x at the breakthrough time 3.96 years when the initial reservoir temperature is 250 °C and the injection temperature is 25 °C

In the above hot water injection case, the initial reservoir temperature is 0 (T_{10} (x, z, t=0) = T_{20} (x, z, t=0) = 0). But in a geothermal case, the initial reservoir temperature T_{10}' is nonzero. To derive the solution from the above solution, substitute T_1 with T_1'-T_{10}' and T_i with T_i'-T_{10}' in *Equation 5*:

$$T_1' - T_{10}' = (T_i' - T_{10}')erfc\left(\frac{\xi}{2\sqrt{\theta(\tau-\xi)}}\right), when\ \tau > \xi \quad (8)$$

T_1' is the reservoir temperature when the initial reservoir

temperature $T_{10}'$is non-zero. Then the solution T_1' with non-zero initial reservoir temperature T_{10}' is:

$$T_1' = T_{10}' + (T_i' - T_{10}')erfc\left(\frac{\xi}{2\sqrt{\theta(\tau-\xi)}}\right), when\ \tau > \xi \quad (9)$$

A geothermal case (cold water injection) is opposite to the hot water injection case, with a low injection temperature T_0' and a high initial reservoir temperature T_{10}', *Equation 9* can be used to predict the temperature distribution.

Using the base model parameters in Table 1 except for the injection temperature T_i'=25 °C, and an initial reservoir temperature T_{10}'= T_{20}' = 250 °C, the temperature distribution along x is shown in Fig. 4. It shows that the temperature of injected fluid (water) is increased towards to the producer. After the breakthrough, the produced fluid temperature decreases with time as shown in Fig. 5.

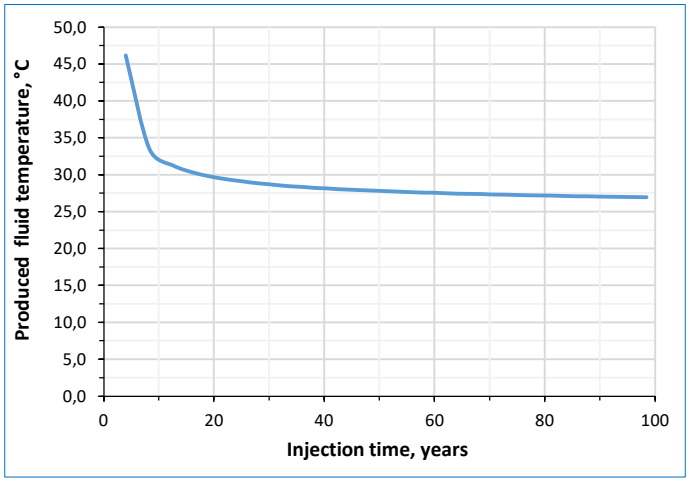

Fig. 5. Temperature at the producer end T_{1L} versus injection time when the initial reservoir temperature is 250 °C and the injected water temperature is 25 °C

For ease of discussion, *Equation 9* is re-written in *Equation 10* with prime removed.

$$T_1 = T_{10} + (T_i - T_{10})erfc\left(\frac{\xi}{2\sqrt{\theta(\tau-\xi)}}\right), when\ \tau > \xi \quad (10)$$

The net heat production rate q_h which is the total produced heat minus the injection fluid heat) is

$$q_h = v_w(2b)w(\rho C)_w(T_{1L} - T_i) \quad (11)$$

where T_{1L} is evaluated using *Equation 10* when $\xi = \xi_L$ at the production end. Or,

$$q_h = q_w C_w(T_{1L} - T_i) \quad (12)$$

where q_w is the injection rate in kg/s, and C_w is the water heat capacity in kJ/(kg·°C).

Before the breakthrough, the heat production rate is constant with the produced fluid temperature at the initial reservoir temperature T_{10}. For ease of study, this heat is not studied here. Note that condition $\tau > \xi$ is valid after the breakthrough. Referring to *Equation 10*, *Equation 11* becomes.

$$q_h = v_w(2b)w(\rho C)_w\Big(T_{10} + (T_i - T_{10})erfc\left(\frac{\xi_L}{2\sqrt{\theta(\tau-\xi_L)}}\right) - T_i\Big) \quad (13)$$

Or *Equation 12* becomes

$$q_h = q_w C_w\left(T_{10} + (T_i - T_{10})erfc\left(\frac{\xi_L}{2\sqrt{\theta(\tau-\xi_L)}}\right) - T_i\right) \quad (14)$$

The net produced heat is shown in Fig. 6. The cumulative heat production Q_h after the breakthrough is from *Equation A-10* in Appendix:

$$\begin{aligned} Q_h &= \int_{t_{bk}}^{t} q_h dt \\ &= q_w C_w(T_{10} - T_i)(t - t_{bk}) \\ &+ q_w C_w \frac{(T_{10} - T_i)b^2(\rho C)_1 {\xi_L}^2}{2\theta\lambda_2}\Bigg\{\Bigg[-\frac{2\theta(\tau-\xi_L)erfc\left(\frac{\xi_L}{2\sqrt{\theta(\tau-\xi_L)}}\right)}{{\xi_L}^2} \\ &+ \frac{1}{\sqrt{\pi}}exp\left(-\frac{{\xi_L}^2}{4\theta(\tau-\xi_L)}\right)\left(\frac{2\sqrt{\theta(\tau-\xi_L)}}{\xi_L}\right) \\ &+ \mathrm{erf}\left(\frac{\xi_L}{2\sqrt{\theta(\tau-\xi_L)}}\right)\Bigg]_{\tau_{bk}}^{\tau}\Bigg\} \end{aligned} \quad (15)$$

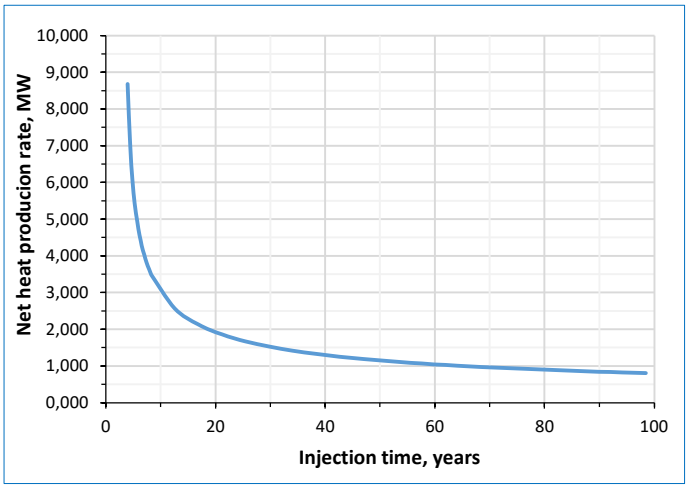

Fig. 6. Net heat production rate after breakthrough when the initial reservoir temperature is 250 °C and the injection temperature is 25 °C

The net cumulative production heat calculated by *Equation 15* is shown in Fig. 7. Alternatively, the *Equation 16*. The result is also demonstrated in Fig. 7. The difference of heat is calculated from *Equations 15 and 16* are almost invisible in Fig. 7. Therefore, the analytical solution *Equation 15* is validated.

$$Q_h(t_n) = Q_h(t_{n-1}) + 0.5 * \left(q_h(t_n) + q_h(t_{n-1})\right) * (t_n - t_{n-1}) \quad (16)$$

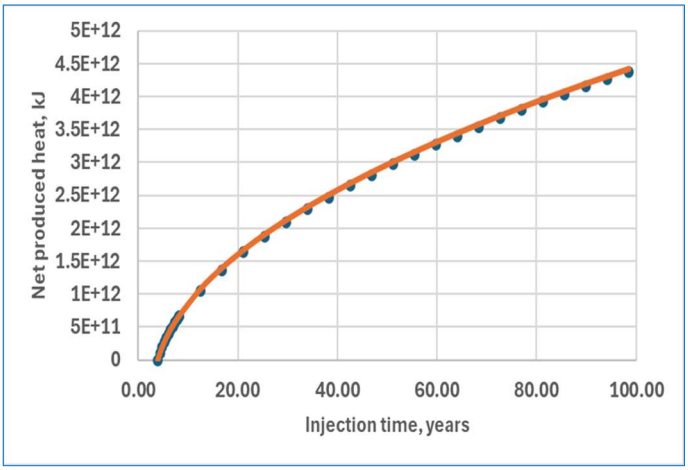

Fig. 7. Net cumulative production heat after breakthrough when the initial reservoir temperature is 250 °C and the injection temperature is 25 °C, calculated from *Equation 15* (line) and from *Equation 16* (dot)

3. Discussion of Results and Their Implications

The results from the preceding base case are first discussed, followed by sensitivity analysis. The implications from the results are discussed in terms of the efficiency of geothermal energy and the design of geothermal projects.

3.1. Base Case

Fig. 5 shows the temperature at the production end versus injection time when the initial reservoir temperature is 250 °C and the injection temperature is 25 °C. It shows that the temperature is increased from 25 to 46 °C after 3.96 years of transport from the injection side to the production in the hot reservoir of 250 °C. After the breakthrough, the temperature quickly drops to 34 °C followed by a long period of low temperatures from 27 to 30 °C. Similarly, Fig. 6 shows that the heat production rate quickly drops after breakthrough and stays at low rates afterwards. Geothermal energy is considered sustainable energy. From the base case results, it is not effective to produce heat by cycling water, as the temperature of the cycled water will be low. If the reservoir is dry or of a low fluid saturation, heat is not produced before the breakthrough. After the breakthrough, the fluid temperature is low.

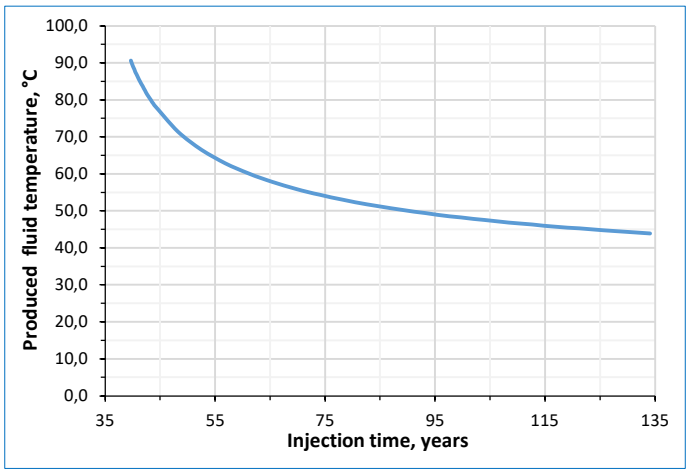

Fig. 8. Temperature at the producer end versus injection time when the injection rate is 10 kg/s

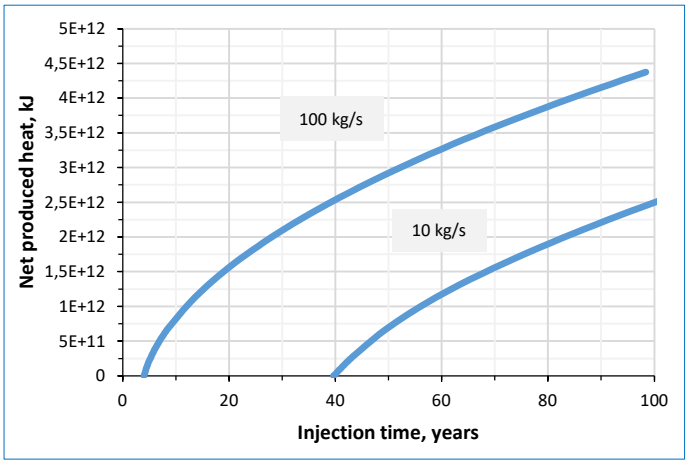

Fig. 9. Net cumulative production heat at the injection rates of 100 kg/s and 10 kg/s

3.2. Effect of Injection Rate

In the base case, the injection rate is 100 kg/s which is about 69,732 bbl/day if the density is assumed 1000 kg/m^3. Such a rate is extremely high for a normal vertical oil well. Even if the injection rate is reduced to 10 kg/s, the equivalent rate of 6,973 bbl/day is high. Under the rate of 10 kg/s, the water velocity in the base model is 0.035 m/day, a low velocity because the model size is large. At such low velocity, the time for the heat transfer from the reservoir to the fluid is long.

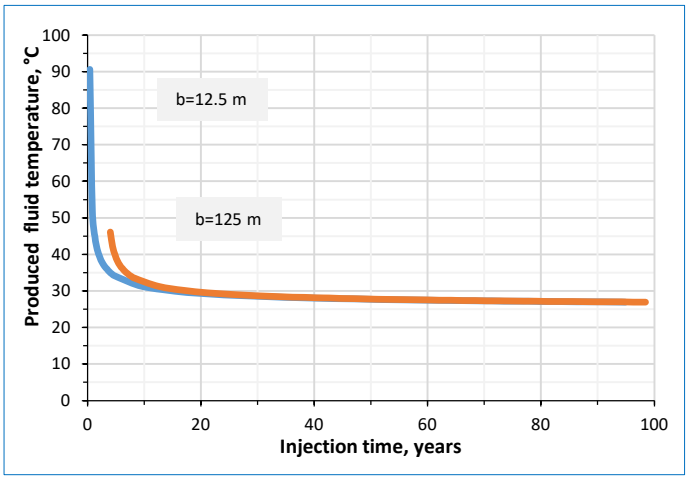

Fig. 10. Temperature at the production end versus injection time when the half formation thickness is 12.5 m and 125 m

Fig. 8 shows that the breakthrough temperature is 91 °C, almost two times that at 100 kg/s rate. In other words, if the rate is reduced by 10 times, the breakthrough temperature is 2 times high. After the breakthrough, the temperature at the producer is within 45 – 60 °C. It is not high compared to the initial reservoir temperature of 250 °C in the model. More importantly, under such a low injection rate, the breakthrough time becomes 39.64 years. Note that no heat can be produced in a dry reservoir before this breakthrough time. Fig. 9 is the net cumulative production heat at the injection rates of 100 kg/s and 10 kg/s. The produced heat at 100 kg/s is almost double the heat at 10 kg/s by 100 years. The important point is that the heat production for the higher

injection rate case is much earlier than that in the low injection rate case. Therefore, reducing injection rate or velocity to increase heating time is not a method to design a geothermal project. Probably, a horizontal well is preferred as it can produce at a high rate but at a low moving velocity.

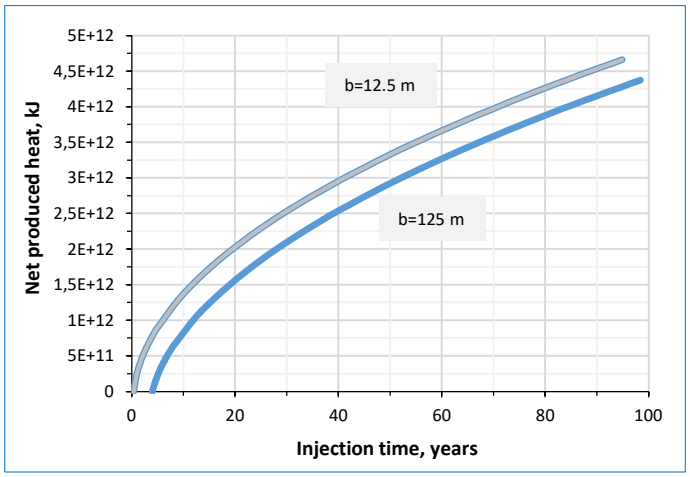

Fig. 11. Net cumulative production heat versus injection time for b = 12.5 m and 125 m

3.3. Effect of Formation Thickness

It is expected that if the formation is thinner, heat can be more easily conducted to heat the injected fluid. In the base case, the formation thickness is 250 m (half thickness b = 125 m). If b is reduced by 10 times to 12.5 m. It is found that the breakthrough temperature is 91 °C as shown on Fig. 10. However, the cumulative heat production is close to each other as shown on Fig. 11.

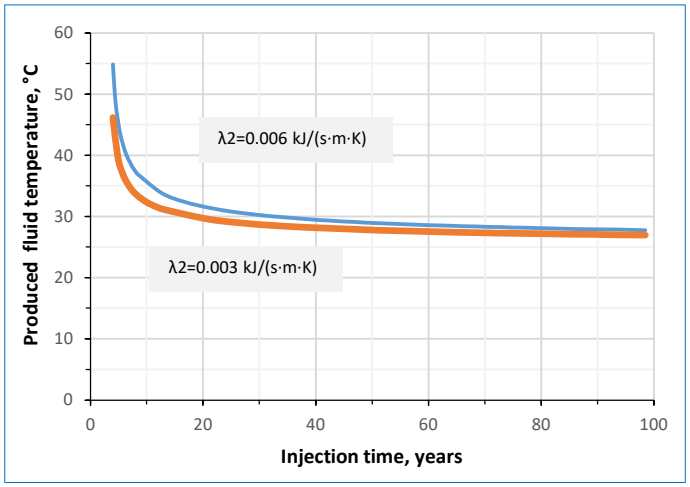

Fig. 12. Temperature at the production end versus injection time when the thermal conductivity values are 0.003 and 0.006 kJ/(s.m.K)

These results indicate that heat transfer rate does not change much with the heated layer thickness for a specific reservoir system, as the heat transfer is through the layer interfaces, and it mainly depends on the area of interfaces, thermal conductivity, and temperature gradient. This is interesting confirmation from these results, which are not expected from oil production. In oil production, a high formation thickness will lead to a high production rate. The formation thickness is not sensitive in geothermal engineering, because a low thickness b requires a high velocity to maintain a reasonably high rate because rate q = vbw, which is not preferred; or, a high thickness b is preferable to a high rate, but not preferable to heat transfer.

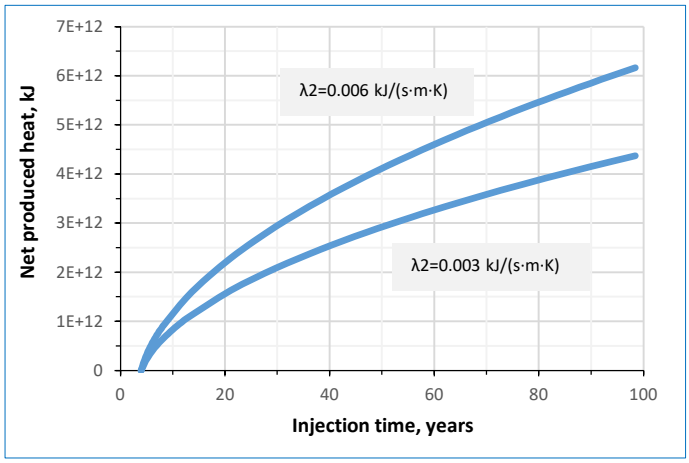

Fig. 13. Net cumulative production heat versus injection time when the thermal conductivity values are 0.003 and 0.006 kJ/(s.m.K)

3.4. Effect of Thermal Conductivity of Over- or Under-Burden λ_2

Obviously, heat transfer can be enhanced if the thermal conductivity of the overburden and underburden λ_2 is high. The value of the base model is 0.003 kJ/(s·m·K). For the high side, the value may be doubled, i.e., 0.006 kJ/(s·m·K). The produced temperatures for the two cases are only quite different in the early times as shown in Fig. 12, where the early temperature ratio of the high case to that of the base case is 1.2. The cumulative produced heat for the high case is about 1.5 times that of the base case at the end of 100 years as shown in Fig. 13, showing the sensitivity of the thermal conductivity. However, the variation of thermal conductivity is limited in practical rock systems.

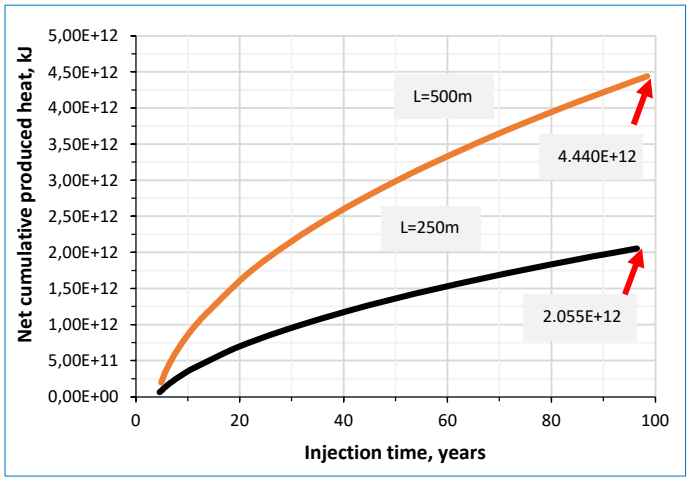

Fig. 14. Net cumulative production heat versus injection time for L = 250 m and 500 m

3.5. Effect of Injector-Producer Distance (well spacing)

If the distance is 250 m, the net cumulative produced heat is

compared in Fig. 14. Overall, the cumulative produced heat in the L250m case is almost half that of the L=500m case. For example, at the end of 100 years, the cumulative heat is 2.055E+12 kJ versus 4.440E+12 kJ (0.46 times). The heat recovery efficiency (factor) defined as the heat produced divided by the original heat within the reservoir) is almost the same. Note that the two cases have the same injection rate. If the injection pressure is the same, the injection rate for the short well spacing case will have a higher rate (about double), then the produced heat might be similar or may not be higher than the corresponding long well spacing case. From this data, long well spacing is preferred when designing a practical project.

3.6. Effect of Injected Fluid Temperature

The injected fluid temperature in the base is 25 °C. If this temperature is raised to 50 °C, the net produced heat is 0.889 times that in the base as shown in Fig. 15, almost same as the base case.

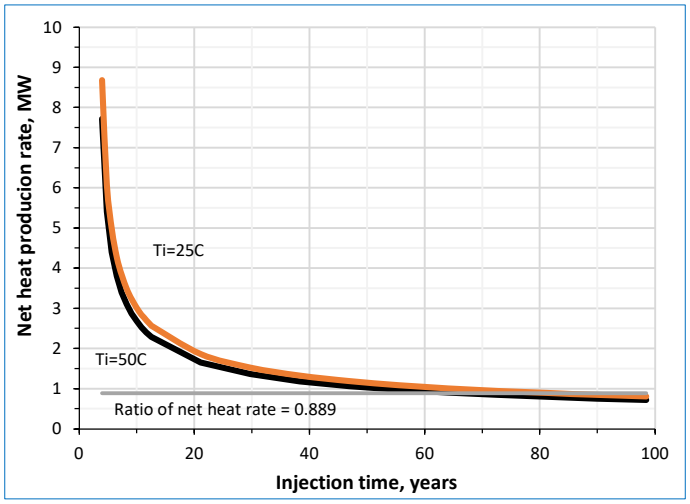

Fig. 15. Net heat production rate versus injection time for Ti = 25 °C and 50 °C

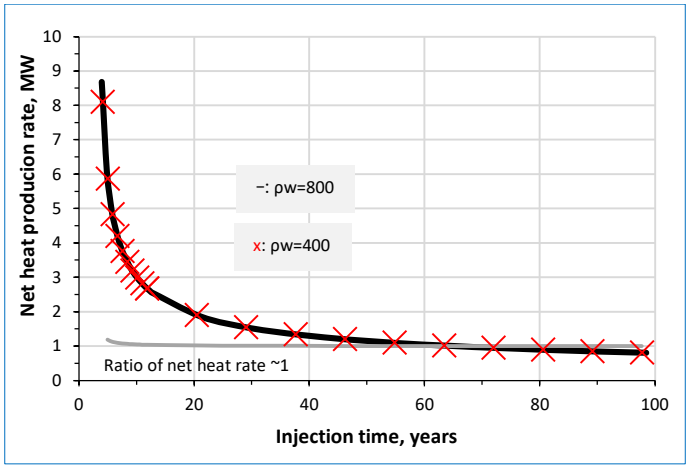

Fig. 16. Net heat production rate versus injection time for water densities = 800 and 400 kg/m^3

3.7. Effect of Water Density

The water density is 800 kg/m^3 in the base. If the water density is reduced, especially in a dry reservoir, some water may be vaporized. The heat rate for the water density reduced by half is compared to the base case in Fig. 16. It shows that the heat rate ratio of the two cases is almost one.

4. Conclusions

If a geothermal reservoir is saturated with fluid, before cold water breaks through the production well, heat is produced. However, in a dry geothermal reservoir, a waiting time for years is needed to produce heat until injected water breaks though.

After breakthrough, the temperature of produced fluid is low compared to the initial reservoir temperature. This questions the effectiveness of cycling water to produce heat as sustainable energy.

To produce geothermal energy, the production rate must be high or much higher than typical oil production.

A low injection rate helps to increase the temperature of produced fluid. However, a low injection rate carries low heat content. Probably, a horizontal well is preferred as it can produce at a high rate but at a low moving velocity.

The formation thickness is not sensitive in geothermal engineering, because a low thickness b requires a high velocity to maintain a reasonably high rate because rate $q = vbw$, which is not preferred; or, a high thickness b is preferable to a high rate, but not preferable to heat transfer.
Thermal conductivity is a sensitive parameter to heat production.

Long well spacing is preferred when designing a practical project.

Injected fluid temperature does not affect the heat production significantly.

Acknowledgements

The work in this paper is supported by these funds: 1. Local Universities Reformation and Development Personnel Training Project from Central Authorities, Study on nano system displacement method of tight reservoir in Daqing Oilfield; 2. Heilongjiang Postdoctoral Scientific Research Fund (LBH-Q21012), Dynamic identification and optimization control of polymer channeling in Class-II oil layer of Daqing Oilfield.

References

Anderson, A., Rezaie, B., 2019. Geothermal technology: Trends and potential role in a sustainable future, Applied Energy 248, 18-34. https://doi.org/10.1016/j.apenergy.2019.04.102.

Bin Sultan, Z., Sheng, J.J., 2025. Strategic approach to EGS working fluid selection: Performance assessment of water and CO_2. Energy 319, 134945. https://doi.org/10.1016/j.energy.2025.134945.

Birhanu, Z.K., Kitterød, N.O., Krogstad, H.E., Kværnø, A., 2023. Analytical and numerical solutions of radially symmetric aquifer thermal energy storage problems. Hydrology Research 54 (11), 1432. https://doi.org/10.2166/nh.2023.214.

Chen, K., Sun, X., Soga, K., Nico, P.S., Dobson, P.F., 2024. Machine-learning-assisted long-term G functions for

bidirectional aquifer thermal energy storage system operation. Energy 301, 131638. https://doi.org/10.1016/j.energy.2024.131638.

Chu, S., Majumdar, A., 2012. Opportunities and challenges for a sustainable energy future. Nature 488, 294-303. https://doi.org/10.1038/nature11475.

Falcone, G., Teodoriu, C., 2008. Oil and gas expertise for geothermal exploitation: The need for technology transfer, paper SPE-113852 presented at Europec/EAGE Conference and Exhibition 2008, June 9-12, Rome, Italy.

Ganguly, S., Kumar, M.M., Abhijit, D., Aliakbar, A., 2015. Numerical Modeling and Analytical Validation for Transient Temperature Distribution in a Heterogeneous Geothermal Reservoir due to Cold-Water Reinjection, Proceedings World Geothermal Congress 2015, 19-25 April, Melbourne, Australia.

June, R., 2013. EGS — Goodbye or Back to the Future 95, From the Proceeding: Effective and Sustainable Hydraulic Fracturing, Edited by Andrew P. Bunger, John McLennan and Rob Jeffrey, https://doi.org/10.5772/56458.

Kelkar, S., WoldeGabriel, G., Rehfeldt, K., 2016. Lessons learned from the pioneering hot dry rock project at Fenton Hill, USA. Geothermics 63, 5-14.

Lauwerier, H.A., 1955. The transport of heat in an oil layer caused by the injection of hot fluid. Applied Scientific Research, Section A 5 (2-3), 145-150. https://doi.org/10.1007/BF03184614.

Martin, J.C., 1975. Analysis of internal steam drive in geothermal reservoirs. Journal of Petroleum Technology 27, 1493-1499. https://doi.org/10.2118/5382-PA.

Ng, E.W., Geller, M., 1969. A table of integrals of the error functions. Journal of Research of the National Bureau of Standards – B. Mathematical Sciences, 73B (1), 1-20. https://doi.org/10.6028/JRES.073B.001.

O'Sullivan, M.J, Pruess, K., Lippmann, M.J., 2001. State of the art of geothermal reservoir simulation. Geothermics 30, 395-429. https://doi.org/10.1016/S0375-6505(01)00005-0.

Pritchett, J.W., 1995. STAR: A geothermal reservoir simulation system, in: Proc. World Geothermal Congress, Florence, 2959–2963.

Pruess, K., Narasimhan, T.N., 1985. A practical method for modeling fluid and heat flow in fractured porous media. Society of Petroleum Engineers Journal 25, 14-26. https://doi.org/10.2118/10509-PA.

Sheng, J.J., 2024. Techno-Economic Analysis of Hydrogen Generation in Hydrocarbon Reservoirs. SPE Journal 29 (10), 5752-5760. https://doi.org/10.2118/223084-PA.

Tadema, H. J., Weijdema, J., 1970. Spontaneous ignition of oil sands. Oil & Gas Journal 68 (50), 77-80.

Zhang, Y., Wu, S., Lu, H., Zha, F., 2025. Analytical solution for temperature-depth in geothermal reservoirs with mixed heat conduction types: A case study from the Huainan Coalfield, Anhui Province, China. Journal of Applied Geophysics 238, 105727. https://doi.org/10.1016/j.jappgeo.2025.105727.

Appendix Derivation of Cumulative Heat Production

The cumulative heat production Q_h after the breakthrough is

$$Q_h = \int_{t_{bk}}^{t} q_h dt = \int_{t_{bk}}^{t} q_w C_w (T_{1L} - T_i) dt = \int_{t_{bk}}^{t} q_w C_w \left(T_{10} + (T_i - T_{10}) erfc\left(\frac{\xi_L}{2\sqrt{\theta(\tau - \xi_L)}} \right) - T_i \right) dt$$
$$= q_w C_w (T_{10} - T_i)(t - t_{bk}) + q_w C_w (T_i - T_{10}) \int_{t_{bk}}^{t} erfc\left(\frac{\xi_L}{2\sqrt{\theta(\tau - \xi_L)}} \right) dt \quad \text{(A-1)}$$

Based on *Equation 6*,

$$d\tau = \frac{\lambda_2 dt}{b^2 (\rho C)_1} \quad \text{(A-2)}$$

the integral term in A-1 becomes

$$\int_{t_{bk}}^{t} erfc\left(\frac{\xi_L}{2\sqrt{\theta(\tau - \xi_L)}} \right) dt = \frac{b^2 (\rho C)_1}{\lambda_2} \int_{\tau_{bk}}^{\tau} erfc\left(\frac{\xi_L}{2\sqrt{\theta(\tau - \xi_L)}} \right) d\tau \quad \text{(A-3)}$$

Let

$$z = \frac{\xi_L}{2\sqrt{\theta(\tau - \xi_L)}} \quad \text{(A-4)}$$

Then

$$d\tau = -\frac{{\xi_L}^2 z^{-3}}{2\theta} dz \quad \text{(A-5)}$$

The integral term in A-3 becomes

$$\int_{t_{bk}}^{t} erfc\left(\frac{\xi_L}{2\sqrt{\theta(\tau-\xi_L)}}\right)dt = \frac{b^2(\rho C)_1}{\lambda_2}\int_{\tau_{bk}}^{\tau} erfc\left(\frac{\xi_L}{2\sqrt{\theta(\tau-\xi_L)}}\right)d\tau = -\frac{b^2(\rho C)_1{\xi_L}^2}{2\theta\lambda_2}\int_{z_{bk}}^{z} erfc(z)\,z^{-3}dz \tag{A-6}$$

According to Ng and Geller (1969),

$$\int erfc(az)z^{-n}dz = -\frac{erfc(az)}{(n-1)z^{n-1}} - \frac{2a}{(n-1)\sqrt{\pi}}\int \frac{1}{z^{n-1}}e^{-a^2z^2}dz\ , \qquad n \geq 2 \tag{A-7}$$

When a = 1, n = 3,

$$\begin{aligned}\int erfc(az)z^{-n}dz &= \int erfc(z)z^{-3}dz = -\frac{erfc(z)}{2z^2} - \frac{1}{\sqrt{\pi}}\int \frac{1}{z^2}e^{-z^2}dz = -\frac{erfc(z)}{2z^2} + \frac{1}{\sqrt{\pi}}\int e^{-z^2}d(z^{-1}) \\ &= -\frac{erfc(z)}{2z^2} + \frac{1}{\sqrt{\pi}}e^{-z^2}z^{-1} + \frac{2}{\sqrt{\pi}}\int e^{-z^2}dz = -\frac{erfc(z)}{2z^2} + \frac{1}{\sqrt{\pi}}e^{-z^2}z^{-1} + \text{erf}\,(z)\end{aligned} \tag{A-8}$$

Put this integral A-8 in A-6, the integral term in A-3 becomes

$$\begin{aligned}&\int_{t_{bk}}^{t} erfc\left(\frac{\xi_L}{2\sqrt{\theta(\tau-\xi_L)}}\right)dt = \frac{b^2(\rho C)_1}{\lambda_2}\int_{\tau_{bk}}^{\tau} erfc\left(\frac{\xi_L}{2\sqrt{\theta(\tau-\xi_L)}}\right)d\tau \\ &= -\frac{b^2(\rho C)_1{\xi_L}^2}{2\theta\lambda_2}\int_{z_{bk}}^{z} erfc(z)\,z^{-3}dz \\ &= \left\{-\frac{b^2(\rho C)_1{\xi_L}^2}{2\theta\lambda_2}\left[-\frac{erfc(z)}{2z^2} + \frac{1}{\sqrt{\pi}}e^{-z^2}z^{-1} + \text{erf}\,(z)\right]\right\}_{z_{bk}}^{z} \\ &= \left\{-\frac{b^2(\rho C)_1{\xi_L}^2}{2\theta\lambda_2}\left[-\frac{2\theta(\tau-\xi_L)erfc\left(\frac{\xi_L}{2\sqrt{\theta(\tau-\xi_L)}}\right)}{{\xi_L}^2} + \frac{1}{\sqrt{\pi}}exp\left(-\frac{{\xi_L}^2}{4\theta(\tau-\xi_L)}\right)\left(\frac{2\sqrt{\theta(\tau-\xi_L)}}{\xi_L}\right)\right.\right. \\ &\qquad \left.\left. + \text{erf}\,\left(\frac{\xi_L}{2\sqrt{\theta(\tau-\xi_L)}}\right)\right]\right\}_{\tau_{bk}}^{\tau}\end{aligned} \tag{A-9}$$

Put this above integral into A-1:

$$\begin{aligned}&Q_h = \int_{t_{bk}}^{t} q_h dt = \int_{t_{bk}}^{t} q_w C_w\left(T_{10} + (T_i - T_{10})erfc\left(\frac{\xi_L}{2\sqrt{\theta(\tau-\xi_L)}}\right) - T_i\right)dt \\ &= q_w C_w(T_{10} - T_i)(t - t_{bk}) + q_w C_w(T_i - T_{10})\int_{t_{bk}}^{t} erfc\left(\frac{\xi_L}{2\sqrt{\theta(\tau-\xi_L)}}\right)dt \\ &= q_w C_w(T_{10} - T_i)(t - t_{bk}) + q_w C_w\frac{(T_{10}-T_i)b^2(\rho C)_1{\xi_L}^2}{2\theta\lambda_2}\left\{\left[-\frac{2\theta(\tau-\xi_L)erfc\left(\frac{\xi_L}{2\sqrt{\theta(\tau-\xi_L)}}\right)}{{\xi_L}^2} + \frac{1}{\sqrt{\pi}}exp\left(-\frac{{\xi_L}^2}{4\theta(\tau-\xi_L)}\right)\left(\frac{2\sqrt{\theta(\tau-\xi_L)}}{\xi_L}\right) + \right.\right. \\ &\left.\left.\text{erf}\,\left(\frac{\xi_L}{2\sqrt{\theta(\tau-\xi_L)}}\right)\right]\right\}_{\tau_{bk}}^{\tau}\end{aligned} \tag{A-10}$$